

Sparse Sensing with Semi-Coprime Arrays

Kaushallya Adhikari

Abstract—A semi-coprime array (SCA) interleaves two under-sampled uniform linear arrays (ULAs) and a Q element standard ULA. The undersampling factors of the first two arrays are QM and QN respectively where M and N are coprime. The resulting non-uniform linear array is highly sparse. Taking the minimum of the absolute values of the conventional beampatterns of the three arrays results in a beampattern free of grating lobes. The SCA offers more savings in the number of sensors than other popular sparse arrays like coprime arrays, nested arrays, and minimum redundant arrays. Also, the SCA exhibits better side lobe patterns than other sparse arrays. An example of direction of arrival estimation with the SCA illustrates SCA's promising potential in reducing number of sensors, decreasing system cost and complexity in various signal sensing and processing applications.

Index Terms—Semi-coprime arrays, sparse arrays, super-resolution, coprime arrays, nested arrays, minimum redundant arrays.

I. INTRODUCTION

MANY linear sparse array designs achieve the resolution of a fully populated uniform linear array (ULA), hereafter called full ULA [1]–[14]. Some of these designs, [1]–[5], use conventional beamforming (CBF) to process the received signal, while some other designs, [6]–[14], split the sparse array into two subarrays and multiply the subarrays' individual CBF outputs. The sparse array designs that existed prior to 2010 suffered from a common limitation — the lack of concrete design criteria or the analytical expressions for the sensor locations. The nested arrays [11], [12] and coprime sensor arrays (CSAs) [13], [14] overcome the limitation by providing analytical expressions for the sensor locations. The generalized coprime array configuration treats the coprime and nested arrays as its special cases [15].

A nested array interleaves a short full ULA with an under-sampled ULA having the same undersampling factor as the number of sensors in the short full ULA. A CSA interleaves two under-sampled subarrays where the undersampling factors are coprime integers. In addition to having convenient analytical expressions for the sensor locations, the NSA and CSA also have a clear mechanism to disambiguate aliasing that occurs due to undersampling. Moreover, the CSAs can also match the peak side lobe height of a full ULA of equal resolution [16] thereby dominating the field of sparse arrays in recent years. The reduction of number of sensors in these sparse arrays translates to lower system cost, and decreased system complexity.

This paper introduces a novel sparse array called semi-coprime array (SCA). The SCA has the potential to offer more reduction in the number of sensors than even the CSA and

the NSA, while still offering the crucial advantages of the CSA and the NSA which are the analytical expressions for the sensor locations, equal resolution as the full ULA with equivalent aperture, and prudent cancellation of the grating lobes resulting from undersampling. The SCA can achieve the peak side lobe height of a full ULA with much less extension than the CSA and the NSA. Since the SCA is sparser than the CSA and the NSA, the SCA suffers less from mutual coupling effect between adjacent sensors than the CSA and the NSA.

Section II describes the SCA in detail. Section III compares the SCA with other popular sparse arrays (CSA, NSA, and minimum redundant arrays). Section IV demonstrates how SCA's inherent super-resolution characteristic can be used in direction of arrival estimation and compares the SCA with other sparse arrays.

Conventions: Bold-faced letters represent vectors; x^* denotes complex conjugate of x ; \mathbf{x}^H denotes Hermitian of \mathbf{x} ; $GCD(a, b)$ denotes the greatest common divisor (GCD) of the integers a and b ; $\min(a, b, c)$ denotes the minimum of a , b , and c .

II. SEMI-COPRIME ARRAYS

This section is going to describe the novel array design and its associated processor in detail.

A. Semi-Coprime Arrays Structure

A semi-coprime array (SCA) is a sparse array that interleaves three ULAs, hereafter called Subarray 1, Subarray 2, and Subarray 3. Each SCA has underlying coprime integers M , and N . Subarray 1 has PM sensors (Symbol \triangle) and $QN \frac{\lambda}{2}$ intersensor spacing, and Subarray 2 has PN sensors (Symbol ∇) and $QM \frac{\lambda}{2}$ intersensor spacing, where P and Q are integers greater than 1, and λ is the wavelength of the signal to be sampled. The Subarray 3 has $\frac{\lambda}{2}$ intersensor spacing and the number of sensors (Symbol \triangleleft) is equal to the GCD of the undersampling factors in the Subarray 1 and Subarray 2, i.e., $Q = GCD(QM, QN)$. Figure 1 depicts the formation of an SCA for $M = 3$, $N = 4$, $P = 2$, and $Q = 2$. The three subarrays always share the first sensor. The Subarray 1 and the Subarray 2 always share P sensors. Hence, the total number of sensors in an SCA is $PM + PN + Q - 1 - P$ but it can achieve the resolution of a full ULA with $PQMN$ sensors. For example, if $P = 2$, $Q = 6$, $M = 4$, and $N = 5$, the SCA has only 21 sensors and it achieves the resolution of a full ULA with 240 sensors.

B. Min Processing

The proposed processor for the SCA is a min processor as depicted in Figure 2. The vectors \mathbf{x}_1 , \mathbf{x}_2 , and \mathbf{x}_3 represent the

This material is based upon research supported by the Louisiana Tech University.

The author is with the Louisiana Tech University, Ruston, LA, 71270 USA. e-mail: adhikari@latech.edu.

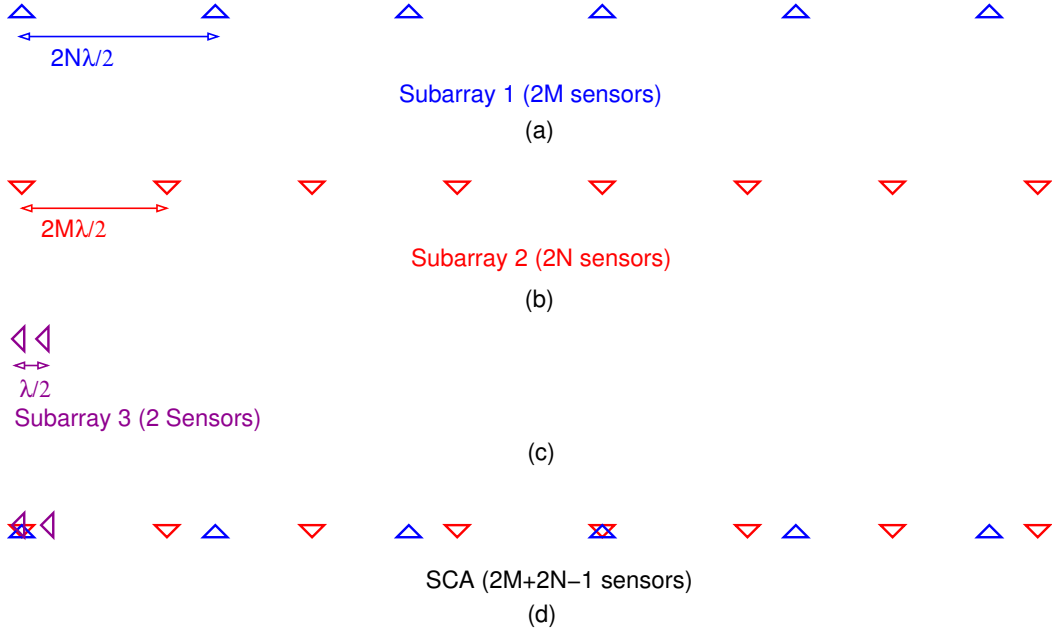


Fig. 1. (a). Subarray 1 with $2M$ sensors and undersampling factor $2N$ (b). Subarray 2 with $2N$ sensors and undersampling factor $2M$ (c). Subarray 3 with 2 sensors and undersampling factor 1 (d). The SCA resulting from interleaving Subarray 1, Subarray 2, and Subarray 3

signal received by the three subarrays. The SCA processor conventionally beamforms each of the three subarrays' received signal by using the weight vectors \mathbf{w}_1 , \mathbf{w}_2 , and \mathbf{w}_3 . Assuming uniform weighting, the vectors \mathbf{w}_1 , \mathbf{w}_2 , and \mathbf{w}_3 are PM , PN , and Q element vectors and their i^{th} elements for direction cosine $u = \cos(\theta)$ are $\frac{1}{PM} \exp(j\pi u(i-1)QN)$, $\frac{1}{PN} \exp(j\pi u(i-1)QM)$, and $\frac{1}{Q} \exp(j\pi u(i-1))$ respectively. The CBF outputs for the three subarrays are $y_1 = \mathbf{w}_1^H \mathbf{x}_1$, $y_2 = \mathbf{w}_2^H \mathbf{x}_2$, and $y_3 = \mathbf{w}_3^H \mathbf{x}_3$. The final SCA output, y , is the minimum of the absolute values of the three CBF outputs, i.e., $y = \min(|y_1|, |y_2|, |y_3|)$.

Although both Subarray 1 and Subarray 2 are undersampled, the SCA output disambiguates aliasing by appropriately combining the Subarray 1, Subarray 2 and Subarray 3 outputs. The Subarray 1 beampattern has the undersampling factor QN , and as a result, it has QN major lobes at integer multiples of $2/(QN)$. Assuming the array is steered to broadside, i.e. $u = \cos(\frac{\pi}{2}) = 0$, the major lobe at $u = 0$ is the main lobe and the other $QN - 1$ major lobes are grating lobes resulting from undersampling. The Subarray 2 beampattern has the undersampling factor QM , and consequently, it has QM major lobes at integer multiples of $2/(QM)$. The major lobe at $u = 0$ is the main lobe and the other $QM - 1$ major lobes are grating lobes due to undersampling. The Subarray 3 beampattern has one major lobe at $u = 0$ which is the main lobe and it has nulls at integer multiples of $2/Q$. Since the undersampling factors of Subarray 1 and Subarray 2 have $GCD(QM, QN) = Q$, only Q major lobes of Subarray 1 overlap with Q major lobes of Subarray 2. One of the overlapping major lobes from each of the Subarray 1 and Subarray 2 is the main lobe at $u = 0$, and the other $Q - 1$ overlapping major lobes from each of the Subarray 1 and Subarray 2 cause aliasing. However, the

Subarray 3 has nulls exactly at the locations where the other two subarrays have overlapping grating lobes. As a result, taking the minimum of the three beampatterns generates a beampattern with no grating lobes at all.

Figure 3 elucidates the beampattern formation mechanism for the SCA shown in Figure 1, assuming the array is steered to the direction $u = 0$. The Subarray 1 beampattern (blue dashed in Figure 3) has the undersampling factor $2N = 8$, and as a result, it has 8 major lobes. The major lobe locations are integer multiples of $1/N$, i.e., $u = -0.75, u = -0.5, u = -0.25, u = 0, u = 0.25, u = 0.5, u = 0.75$, and $u = \pm 1$. The major lobe at $u = 0$ is the main lobe and the other 7 major lobes are grating lobes resulting from undersampling. The Subarray 2 beampattern (red dashed-dot in Figure 3) has the undersampling factor $2M = 6$, and consequently, it has 6 major lobes. The major lobe locations are integer multiples of $1/M$, i.e., $u = -0.67, u = -0.33, u = 0, u = 0.33, u = 0.67$, and $u = \pm 1$. The major lobe at $u = 0$ is the main lobe and the other 5 major lobes are grating lobes due to undersampling. The Subarray 3 beampattern (purple dot in Figure 3) has one major lobe at $u = 0$ which is the main lobe. Since the undersampling factors of Subarray 1 and Subarray 2 have $GCD(QM, QN) = 2$, two major lobes of Subarray 1 overlap with two major lobes of Subarray 2. One of the overlapping major lobes from each of the Subarray 1 and Subarray 2 is the main lobe at $u = 0$, and the other overlapping major lobe from each of the Subarray 1 and Subarray 2 is the grating lobe at $u = \pm 1$. However, the Subarray 3 has nulls exactly at $u = \pm 1$. Therefore, taking the minimum of the three beampatterns shown in Figure 3 results in a beampattern (black solid in Figure 3) that is devoid of grating lobes.

Figure 4 compares an SCA beampattern with a standard ULA that offers the same resolution. The standard ULA (green dashed in Figure 4) has 48 sensors while the SCA (black solid

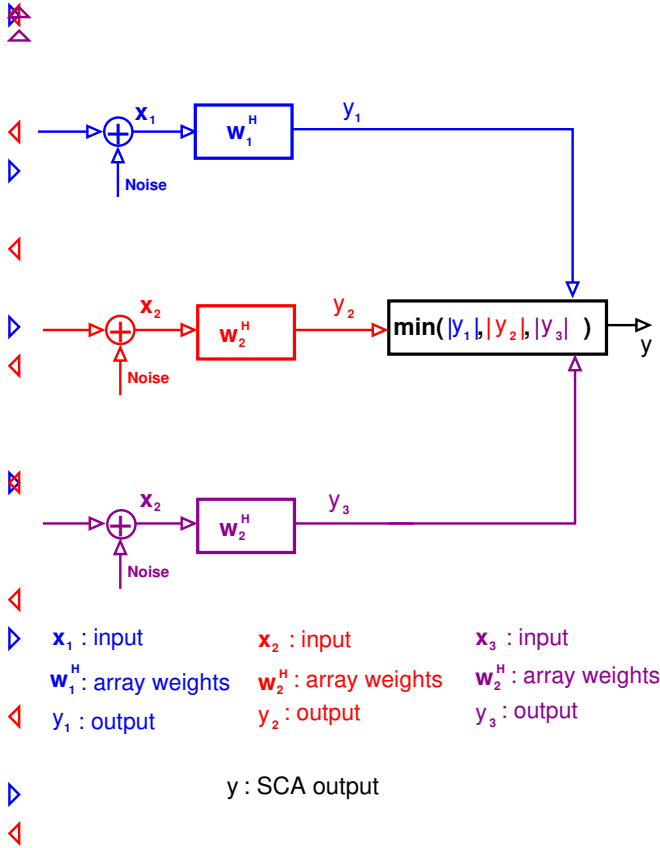


Fig. 2. The SCA min processor conventionally beamforms the Subarray 1 (blue), Subarray 2 (red) and Subarray 3 (purple) data and finds the minimum of the absolute values of the CBF outputs to produce the final output.

in Figure 4) has only 13 sensors. The SCA and the standard ULA have equal main lobe widths and hence equal resolution, and almost equal peak side lobe (PSL) heights. Using only about 27% of the sensors in the standard ULA, the SCA is able to match both resolution and PSL height of the standard ULA, offering a substantial saving in the number of sensors.

III. COMPARISON WITH OTHER SPARSE ARRAYS

As noted in the introduction, many authors have proposed various sparse array schemes over the course of the last few decades. However, the introduction of the NSA and CSA in 2010 and 2011 has sparked renewed interest in sparse arrays. The CSA and NSA have drawn great attention from researchers since they possess concrete expressions for sensor locations and their exists a clear mechanism to remove prudently any grating lobes that arise due to undersampling. Another category of arrays, minimum redundant arrays (MRAs), has also been a relevant topic of research and reference in the field of sparse arrays for several decades. This section summarizes three different versions of the CSA (basic CSA, extended CSA, and min-processing CSA), the NSA, and the MRA and compare them with the novel array, SCA.

1) *Basic Coprime Sensor Array*: A basic CSA is a sparse array that interleaves two ULAs, hereafter called Subarray 1, and Subarray 2. Each CSA has underlying coprime integers M , and N . The Subarray 1 has M sensors (Symbol \triangle in

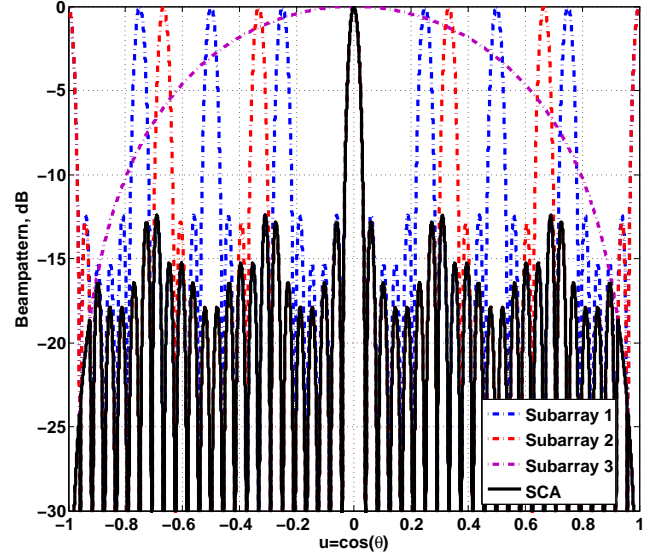


Fig. 3. Formation of the SCA beampattern. Taking the minimum of the absolute values of the Subarray 1 (blue dashed-dot), Subarray 2 (red dashed-dot) and Subarray 3 (purple dashed-dot) beampatterns results in a beampattern (black solid) free of grating lobes.

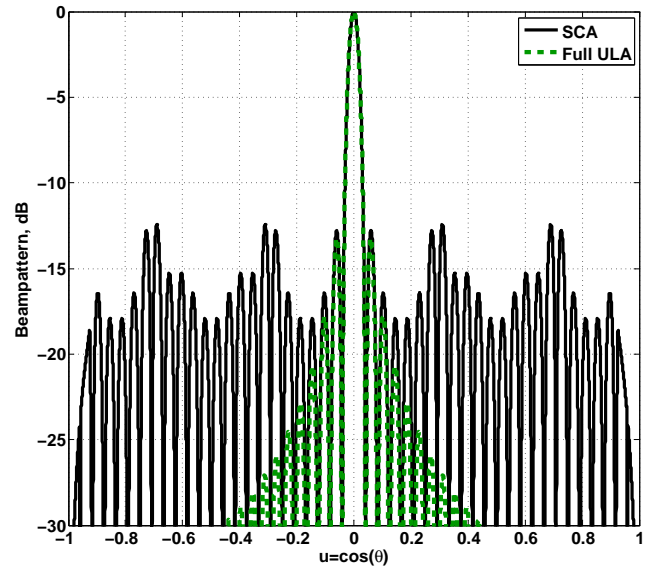


Fig. 4. Comparison of the SCA (black solid), and ULA (green dashed) beampatterns. The two beampatterns have equal main lobe with and PSL height.

Figure 5) and $N\frac{\lambda}{2}$ intersensor spacing, and the Subarray 2 has N sensors (Symbol ∇ in Figure 5) and $M\frac{\lambda}{2}$ intersensor spacing. The total number of sensors in a basic CSA is $M + N - 1$ but it can achieve the resolution of a full ULA with MN sensors [13], [14]. Figure 5 depicts the formation of a basic CSA for $M = 4$, and $N = 5$. The basic CSA has only 8 sensors and it achieves the resolution of a full ULA with 20 sensors. For a CSA with a given aperture, the coprime pair M and $N = M + 1$ minimizes the total number of sensors

needed to span that aperture [16], [17]. This paper assumes that $N = M + 1$.

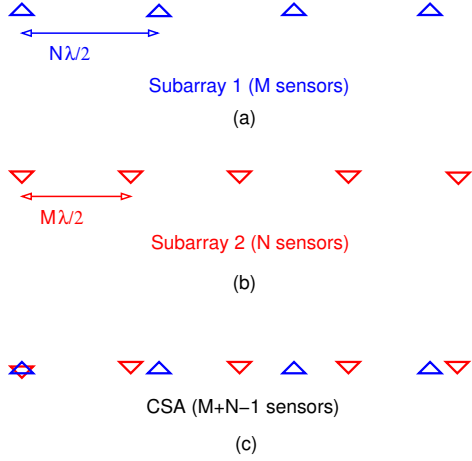


Fig. 5. (a) Subarray 1 (blue) of a CSA with coprime pair (4, 5) (2) Subarray 2 (red) of a CSA with coprime pair (4, 5) (c) The resulting CSA formed by interleaving Subarray 1 and Subarray 2.

A CSA processor eliminates the grating lobes by taking the product of the CBF beampatterns of the two subarrays. The Subarray 1 beampattern has the undersampling factor N , and as a result, it has N major lobes at integer multiples of $2/N$. The major lobe at $u = 0$ is the main lobe and the other $N - 1$ major lobes are grating lobes due to undersampling. The Subarray 2 beampattern has the undersampling factor M , and as a result, it has M major lobes at integer multiples of $2/M$. The major lobe at $u = 0$ is the main lobe and the other $M - 1$ major lobes are grating lobes due to undersampling. Since M and N are coprime, all the grating lobe locations are unique while the main lobes of the Subarray 1 and Subarray 2 are exactly at the same location. Taking the product of the two beampatterns removes the grating lobes.

Figure 6 illustrates the formation of a CSA beampattern for the arrays shown in Figure 5. The CSA has total 8 sensors and the ULA has 20 sensors. However, they have the equal main lobe width and therefore, have equal resolution. Comparing the CSA and the ULA beampatterns also shows that the CSA peak side lobe (PSL) height is much higher than the ULA PSL height. The ULA PSL height is -13 dB while the CSA PSL height is about -4 dB in Figure 6.

2) *Extended Coprime Sensor Array*: As noted in Section III-1, the PSL height of a basic CSA is too high for it to be considered useful in major applications. Keeping the intersensor spacings of the subarrays fixed and adding more sensors to both subarrays causes the CSA PSL to decrease and match the ULA PSL height [13], [14]. The number of additional sensors required to be added to the subarrays to match the PSL height of a standard ULA depends on the coprime factors and the weighting functions used. The derivation of the number of additional sensors for various standard uniform and non-uniform weighting functions exists in [17]. The coprime sensor array where the subarrays have been extended to match the PSL height of the full ULA with the equivalent aperture is called the extended coprime sensor array (ECSA). The numbers of sensors in the Subarray 1

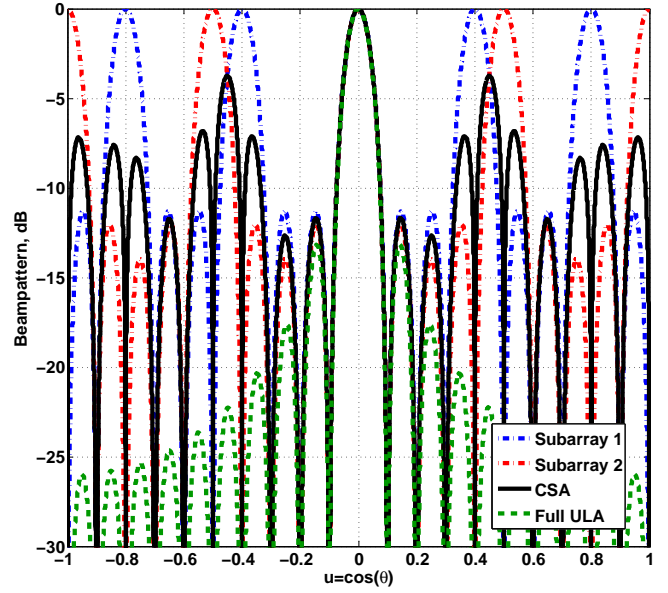


Fig. 6. Subarrays, CSA and full ULA beampatterns.

and Subarray 2 are $M_e = \lceil cN \rceil - 1$ and $N_e = \lceil cN \rceil$. The constant c is called the extension factor which is the number of repetitions of the basic CSA in an ECSA. For uniform shading, the total number of sensors in an ECSA is $L = 13M + 6$ and the ECSA has the resolution of a full ULA with $M_e N$ sensors (See Appendix A).

3) *Min-processing Coprime Sensor Array*: Taking the minimum of the two CBF beampatterns in a basic CSA or an ECSA also removes the grating lobes since the grating lobes are at different locations [18]–[20]. A CSA where each subarray has two periods of the basic subarrays and the associated processor is the min-processor explained in [18]–[20] is, subsequently, called min-processing coprime sensor array (MCSA). An MCSA has $4M$ sensors and it achieves the resolution of a full ULA with $2MN$ sensors (See Appendix B).

4) *Nested Sensor Array*: A nested sensor array (NSA) is a sparse array that interleaves two ULAs, hereafter called Subarray 1, and Subarray 2. The Subarray 1 has M sensors (Symbol \triangle in Figure 7) and $\frac{\lambda}{2}$ intersensor spacing, and Subarray 2 has N sensors (Symbol ∇ in Figure 7) and $M\frac{\lambda}{2}$ intersensor spacing. The total number of sensors in an NSA is $M + N - 1$ but it can achieve the resolution of a full ULA with MN sensors. Figure 7 depicts the formation of an NSA for $M = 5$, and $N = 3$. The NSA has only 7 sensors and it achieves the resolution of a full ULA with 15 sensors.

An NSA processor eliminates the grating lobes by taking the product of the CBF beampatterns of the two subarrays. The Subarray 1 beampattern has only one major lobe at $u = 0$ and it is the main lobe. The Subarray 1 has nulls at integer multiples of $2/M$. The Subarray 2 beampattern has the undersampling factor M , and as a result, it has M major lobes at integer multiples of $2/M$. The major lobe at $u = 0$ is the main lobe and the other $M - 1$ major lobes are grating lobes due to undersampling. Since the grating lobes of the Subarray 2 are exactly at the nulls of the Subarray 1, taking the product

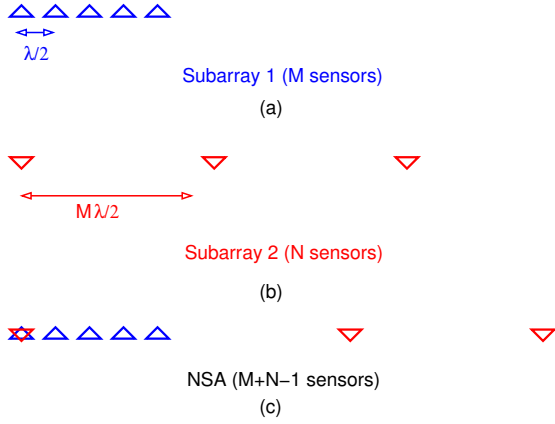


Fig. 7. (a) Subarray 1 (blue) of an NSA with $M = 5$ and $N = 3$ (2) Subarray 2 (red) of an NSA with $M = 5$ and $N = 3$ (c) The resulting NSA.

of the two beampatterns removes the grating lobes.

Figure 8 illustrates the formation of an NSA beampattern for the arrays shown in Figure 7. The NSA has total 7 sensors and the ULA has 15 sensors. However, they have the equal main lobe width and therefore, have equal resolution. Comparing the NSA and the ULA beampatterns also shows that the NSA PSL height is much higher than the ULA PSL height. Extending the NSA subarrays like in CSA does not decrease the NSA PSL height to the level of the full ULA.

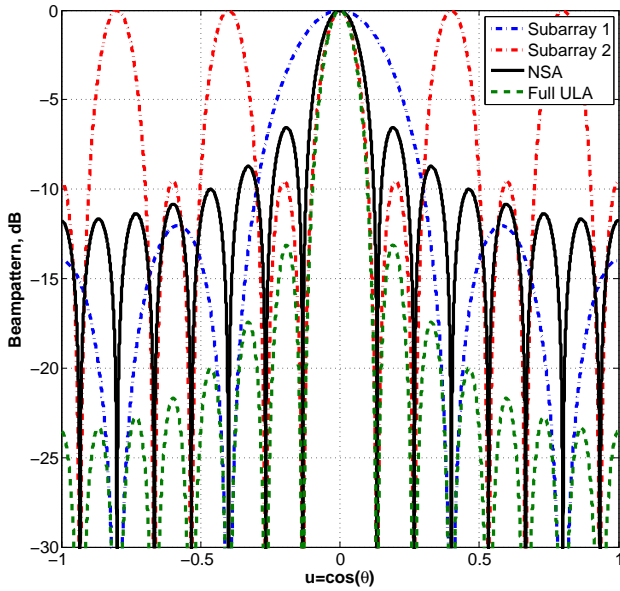


Fig. 8. Subarrays, nested and full ULA beampatterns

5) *Minimum Redundant Array*: Minimum redundant arrays is a class of sparse arrays designed to have the least redundancy in the coarray [21, page 179]. For a given number of sensors, an MRA attains the largest possible hole-free coarray while at the same time, minimizes the number of sensor pairs leading to the same spatial correlation lag. MRAs are the sparsest arrays among arrays that achieve hole-free coarrays. [21, page 182] lists the sensor locations for up to 17 sensors. These sensor locations were obtained through

exhaustive search routines and the analytical expressions for the sensor locations do not exist.

TABLE I
Comparison of the numbers of sensors relative to the full ULA with the equal resolution

Array	Number of sensors	Matches ULA's PSL height?
ECSEA	$\frac{2}{N} \left(\frac{13M+6}{13M+11} \right)$	Yes
Basic CSA	$\frac{2}{N}$	No
MCSA	$\frac{2}{N}$	Yes
NSA	$\frac{2}{N}$	No
SCA	$\frac{2}{N} \left(\frac{PM+0.5Q-0.5}{PQM} \right)$	Yes

6) *Comparison of SCA with CSA, NSA, and MRA*: A sparse array achieves the resolution of a full ULA using fewer sensors. In addition to matching the resolution, some sparse arrays can match the PSL height of a full ULA. For a given resolution, the ratio of the number of sensors in the sparse array to the number of sensors in the full ULA provides a measure of the savings in sensors. The lower ratios indicate more savings in sensors. Table I lists the ratios of the total numbers of sensors of the sparse arrays to the total number of sensors of the full ULA with equal resolution (See Appendix C). The achievable ratio of the numbers of sensors is equal to $\frac{2}{N}$ for the basic CSA, MCSA, and NSA. For the ECSEA, the achievable ratio is $\frac{2}{N} \left(\frac{13M+6}{13M+11} \right)$ which is less than $\frac{2}{N}$ for any M . For the SCA, the achievable ratio is $\frac{2}{N} \left(\frac{PM+0.5Q-0.5}{PQM} \right)$ which is also less than $\frac{2}{N}$ for any M . To realize the super-resolution feature embedded in the SCA, consider fixing the number of sensors to $L = 32$. An ECSEA with $M = 2$ has 32 sensors and it can match both the resolution and the PSL height of a 57 sensor full ULA using only 32 sensors. An MCSA with $M = 8$ has 32 sensors and it can match both the resolution and the PSL height of a 144 sensor full ULA using only 32 sensors. A basic CSA with $M = 16$ has 32 sensors and it can match the resolution of a 272 sensor full ULA, but its PSL height is about -5.5 dB which is much higher than the full ULA (-13 dB). An NSA with $M = 16$ and $N = 17$ also has 32 sensors and it can match the resolution of a 272 sensor full ULA, but its PSL height is much higher than the full ULA. On the other hand, an SCA with $P = 4$, $Q = 9$, $M = 3$ and $N = 4$ has 32 sensors and it can match both the resolution and the PSL of a 432 sensor full ULA using only 32 sensors. Hence, for a fixed number of sensors, the SCA achieves higher resolution than the other sparse arrays and at the same time, matches the PSL height of the full ULA.

Consider a minimum redundant array with number of sen-

sors $L = 17$. This MRA can achieve the resolution of a 102 sensor full array. An SCA with $P = 3$, $Q = 6$, $M = 2$, and $N = 3$ has 17 sensors and it can achieve the resolution of a 102 sensor full ULA. Hence, the SCA offers even more sparsity than the MRA. Moreover, the SCA exhibits better side lobe patterns than the MRA. The beampatterns of the SCA and MRA with 17 sensors are shown in Figure 9. The PSL height of the SCA is -13 dB whereas the PSL height of the MRA is -6.1 dB as evident in Figure 9.

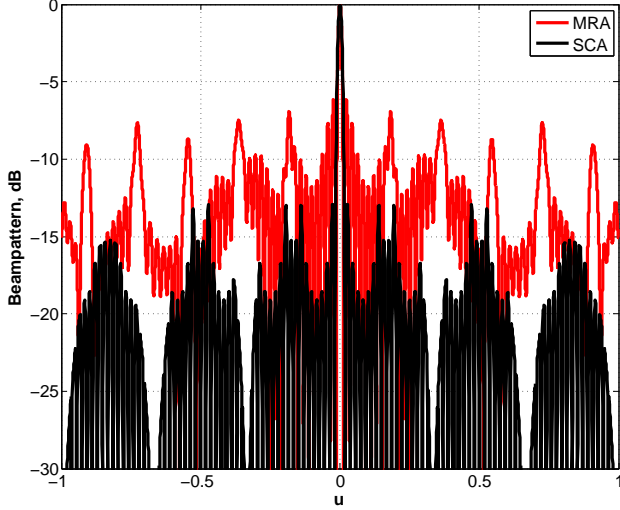


Fig. 9. Comparison of the MRA (red) and SCA (black) beampatterns. The two beampatterns exhibit equal main lobe width, however MRA's PSL height is much higher.

IV. ESTIMATION WITH INCREASED DEGREES OF FREEDOM

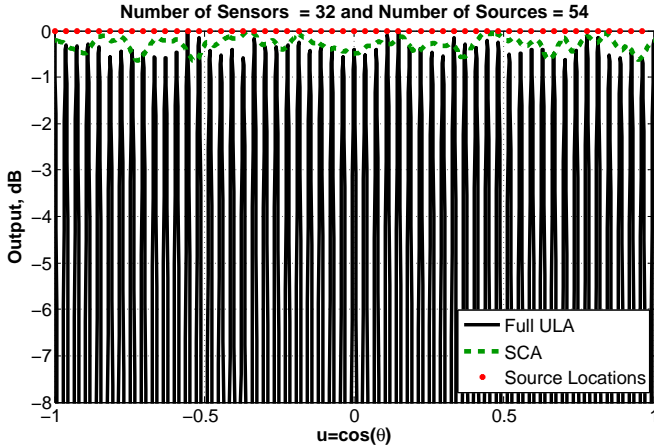


Fig. 10. DoA estimation comparison between an SCA (black solid) with parameters $M = 3$, $N = 4$, $P = 5$, $Q = 3$ and a ULA (green dashed) with the equal resolution. Number of Sensors = 32, Number of Sources = 54, Number of Snapshots = 100 $SNR = 0$ dB

This section demonstrates SCA's ability to detect remarkably more sources than the number of sensors, and compares SCA's direction-of-arrival (DoA) estimation with the other sparse arrays briefed in Section III. In all examples, the total

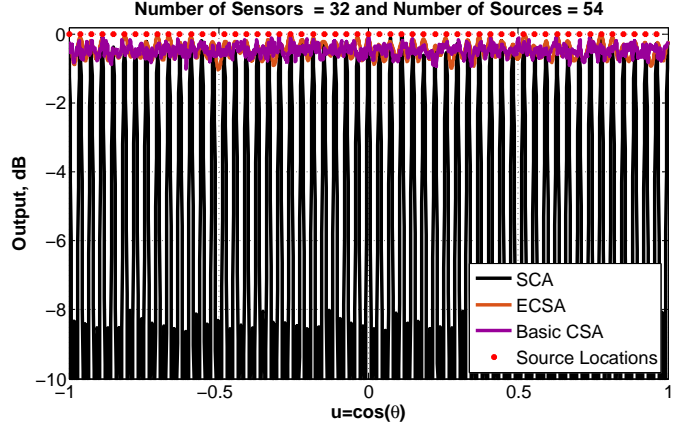


Fig. 11. DoA estimation comparison between an SCA (black solid) with parameters $M = 3$, $N = 4$, $P = 5$, $Q = 3$ and an ECSA (brown solid) with parameters $M_e = 19$, $N_e = 20$, $M = 2$, $N = 3$, $c = 6.5$ and a basic CSA (purple solid) with parameters $M = 16$, $N = 17$. Number of Sensors = 32, Number of Sources = 54, Number of Snapshots = 100 $SNR = 0$ dB

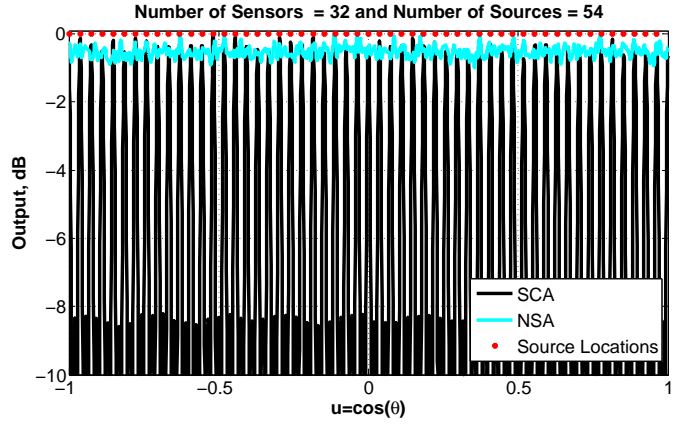


Fig. 12. DoA estimation comparison between an SCA with parameters $M = 3$, $N = 4$, $P = 5$, $Q = 3$ and an NSA (cyan solid) with parameters $M = 10$, $N = 23$. Number of Sensors = 32, Number of Sources = 54, Number of Snapshots = 100 $SNR = 0$ dB

number of sensors L is 32, the number of sources is 54, the number of snapshots is 100, and SNR is 0 dB.

Figure 10 compares DoA estimation by an SCA (black solid line) with parameters $M = 3$, $N = 4$, $P = 5$, $Q = 3$ with a full ULA (green dashed line). The 54 source locations are marked by red circles in the figure. The SCA is able to detect all 54 sources correctly. The full ULA cannot detect any source clearly in this example. Similarly, Figure 11 compares DoA estimation by an SCA with an ECSA ($M_e = 19$, $N_e = 20$, $M = 2$, $N = 3$, $c = 6.5$), and a basic CSA ($M = 16$, $N = 17$). The SCA is able to identify all 54 sources, whereas the CSAs fail to do so. Finally, Figure 12 compares DoA estimation by an SCA with an NSA with $M = 10$ and $N = 23$. The SCA detects 54 sources using only 32 sensors, whereas the NSA does not. Hence, the degrees of freedom offered relative to the numbers of sensors is much higher in

the SCA than in the other sparse arrays.

V. CONCLUSION

This paper introduced a novel sparse array called semi-coprime array, formed by interleaving three subarrays — Subarray 1, Subarray 2, and Subarray 3. Subarray 1 and Subarray 2 have undersampling factors QN and QM , where M and N are coprime integers and Q is the number of sensors in Subarray 3. Min-processing the CBF beam patterns of the three subarrays removes the grating lobes from Subarray 1 and Subarray 2 that are at different locations, while the grating lobes that are at the same locations are suppressed by the nulls of Subarray 3. The resulting non-uniform sparse linear array offers more savings in the number of sensors than other sparse counterparts like coprime arrays, nested arrays, and minimum redundant arrays. Moreover, the SCA matches the PSL height of a full ULA more easily.

The super-resolution feature offered by the SCA can be exploited in applications that involve sensing and processing signals, for example signal estimation and detection. The examples presented in Section IV shows that the SCA has the potential to offer much higher degrees of freedom relative to its number of sensors than possible with other existing sparse arrays, and this could lead to significant reduction in system cost and complexity.

APPENDIX A

TOTAL NUMBER OF SENSORS AND RESOLUTION OF A UNIFORMLY SHADED ECSA

For an ECSA, the numbers of sensors in the Subarray 1 and Subarray 2 are $M_e = \lceil cN \rceil - 1$ and $N_e = \lceil cN \rceil$, where c is the smallest positive number that guarantees ECSA's PSL is less than or equal to -13 dB. Since the subarrays share $\lceil c \rceil$ sensors, the total number of sensors in the array is

$$\begin{aligned} L &= \lceil 2cN - 1 - c \rceil \\ &= \lceil 13N - 1 - 6.5 \rceil \text{ since } c = 6.5 \text{ for uniform shading [17]} \\ &= \lceil 13N - 7.5 \rceil \\ &= \lceil 13M + 13 - 7.5 \rceil \text{ since } N = M + 1. \end{aligned}$$

Hence, the total number of sensors is $L = 13M + 6$.

Since the Subarray 1 has M_e sensors and the intersensor spacing $N \frac{\lambda}{2}$, the main lobe width of its CBF beam pattern is $\frac{4}{M_e N}$. Since the Subarray 2 has M_e sensors and the intersensor spacing $M \frac{\lambda}{2}$, the main lobe width of its CBF beam pattern is $\frac{4}{N_e M}$. The product of the two CBF beam patterns has the

main lobe width

$$\begin{aligned} MLW &= \min \left(\frac{4}{M_e N}, \frac{4}{N_e M} \right) \\ &= \min \left(\frac{4}{(cN - 1)(M + 1)}, \frac{4}{cNM} \right) \\ &= \min \left(\frac{4}{cNM + cN - (M + 1)}, \frac{4}{cNM} \right) \\ &= \min \left(\frac{4}{cNM + c(M + 1) - (M + 1)}, \frac{4}{cNM} \right) \\ &= \frac{4}{cNM + c(M + 1) - (M + 1)} \text{ since } c > 1. \end{aligned}$$

Hence, the main lobe width of the ECSA beam pattern is equal to the main lobe width of the Subarray 1, $\frac{4}{M_e N}$.

APPENDIX B

TOTAL NUMBER OF SENSORS AND RESOLUTION OF AN MCSA

For an MCSA, when the numbers of sensors in the Subarray 1 and Subarray 2 are $M_e = 2M$ and $N_e = 2N$, the PSL height is close to -13 dB. The total number of sensors in an MCSA with $N = M + 1$, $M_e = 2M$ and $N_e = 2N$ is $L = 2M + 2N - 2 = 4M$. Each subarray has the main lobe width of $\frac{4}{2MN}$. Hence, the MCSA has the resolution equal to a full ULA with $2MN$ sensors.

APPENDIX C

RATIOS OF THE NUMBERS OF SENSORS IN THE SPARSE ARRAYS TO THE FULL ULA

For an ECSA, the total number of sensors is $13M + 6$ and it has the resolution of a full ULA with $M_e N$ sensors. Therefore, the ratio of the numbers of sensors in the ECSA to the full ULA is

$$\begin{aligned} R &= \frac{13M + 6}{M_e N} = \frac{2}{N} \frac{13M + 6}{2M_e} \\ &= \frac{2}{N} \frac{13M + 6}{(13N - 2)} \text{ since } M_e = \lceil 6.5N \rceil - 1 \\ &= \frac{2}{N} \frac{13M + 6}{(13M + 11)} \text{ since } N = M + 1 \end{aligned}$$

For a basic CSA, the total number of sensors is $M + N - 1 = 2M$ and it has the resolution of a full ULA with MN sensors. Therefore, the ratio of the numbers of sensors in the basic CSA to the full ULA is $R = \frac{2M}{MN} = \frac{2}{N}$.

For an MCSA, the total number of sensors is $2M + 2N - 2 = 4M$ and it has the resolution of a full ULA with $2MN$ sensors. Therefore, the ratio of the numbers of sensors in the MCSA to the full ULA is $R = \frac{4M}{2MN} = \frac{2}{N}$.

For an NSA, the total number of sensors is $M + N - 1$ and it has the resolution of a full ULA with MN sensors. Therefore, the ratio of the numbers of the sensors in the NSA to the full ULA is $R = \frac{M + N - 1}{MN}$. Assume $N = M - 1$ for the ease of comparison with the other sparse arrays, which will result in $R = \frac{2}{N}$.

For an SCA, the total number of sensors is $PM + PN + Q - P - 1$ and with $N = M + 1$, the number of sensors is $2PM + Q - 1$ and it has the resolution of a full ULA with $PQMN$ sensors. Therefore, the ratio of the numbers of sensors in the SCA to the full ULA is $R = \frac{2PM + Q - 1}{PQMN} = \frac{2}{N} \frac{PM + 0.5Q - 0.5}{PQM}$

ACKNOWLEDGMENT

The author would like to thank John R. Buck for helpful feedback on this research.

REFERENCES

- [1] D. King, R. Packard, and R. Thomas, "Unequally spaced broad-band antenna arrays," *IRE Trans. Antennas Propag.*, vol. AP-8, pp. 380–385, July 1960.
- [2] H. Unz, "Linear arrays with arbitrarily distributed elements," *IRE Trans. Antennas Propag.*, vol. AP-8, pp. 222–223, March 1960.
- [3] A. Ishimaru, "Theory of unequally spaced arrays," *IRE Trans. Antennas Propag.*, vol. AP-10, pp. 691–702, November 1962.
- [4] A. Ishimaru and Y. Chen, "Thinning and broadbanding antenna arrays by unequal spacings," *IRE Trans. Antennas Propag.*, vol. AP-13, pp. 34–42, January 1965.
- [5] A. Moffet, "Minimum-redundancy linear arrays," *IRE Trans. Antennas Propag.*, vol. 16, pp. 172–175, March 1968.
- [6] B. Steinberg, *Principles of aperture and array system design: including random and adaptive arrays*, ser. A Wiley-Interscience publication. John Wiley and Sons Canada, Limited, 1976.
- [7] A. Berman and C. S. Clay, "Theory of time averaged product arrays," *The Journal of the Acoustical Society of America*, vol. 29, no. 7, 1957.
- [8] D. Davies and C. Ward, "Low sidelobe patterns from thinned arrays using multiplicative processing," *IEE Proceedings F Communications, Radar and Signal Processing*, vol. 127, no. 1, pp. 9–23, February 1980.
- [9] G. Kefalas, "An aperture distribution technique for product-array antennas," *IEEE Transactions on Antennas and Propagation*, vol. 16, no. 1, pp. 125–125, January 1968.
- [10] S. Mitra, K. Mondal, M. Tchobanou, and G. Dolecek, "General polynomial factorization-based design of sparse periodic linear arrays," *IEEE Transactions on Ultrasonics, Ferroelectrics, and Frequency Control*, vol. 57, no. 9, pp. 1952–1966, September 2010.
- [11] P. Pal and P. Vaidyanathan, "Nested arrays: A novel approach to array processing with enhanced degrees of freedom," *IEEE Transactions on Signal Processing*, vol. 58, no. 8, pp. 4167–4181, August 2010.
- [12] —, "Nested arrays in two dimensions, part I: Geometrical considerations," *IEEE Transactions on Signal Processing*, vol. 60, no. 9, pp. 4694–4705, September 2012.
- [13] P. Vaidyanathan and P. Pal, "Sparse sensing with co-prime samplers and arrays," *IEEE Transactions on Signal Processing*, vol. 59, no. 2, pp. 573–586, February 2011.
- [14] —, "Theory of sparse coprime sensing in multiple dimensions," *IEEE Transactions on Signal Processing*, vol. 59, no. 8, pp. 3592–3608, August 2011.
- [15] S. Qin, Y. Zhang, and M. Amin, "Generalized coprime array configurations for direction-of-arrival estimation," *IEEE Transactions on Signal Processing*, vol. 63, pp. 1377–1390, March 2015.
- [16] K. Adhikari, J. Buck, and K. Wage, "Beamforming with extended coprime sensor arrays," *2013 IEEE International Conference on Acoustics, Speech and Signal Processing (ICASSP)*, pp. 4183–4186, May 2013.
- [17] —, "Extending coprime sensor arrays to achieve the peak side lobe height of a full uniform linear array," *EURASIP Journal on Advances in Signal Processing*, vol. 2014, no. 1, p. 148, Sep 2014. [Online]. Available: <https://doi.org/10.1186/1687-6180-2014-148>
- [18] Y. Liu and J. Buck, "Detecting gaussian signals in the presence of interferers using the coprime sensor arrays with the min processor," *2015 49th Asilomar Conference on Signals, Systems and Computers*, pp. 370–374, Nov 2015.
- [19] —, "Super-resolution doa estimation using a coprime sensor array with the min processor," *2016 50th Asilomar Conference on Signals, Systems and Computers*, pp. 944–948, Nov 2016.
- [20] —, "Spatial spectral estimation using a coprime sensor array with the min processor," *2016 IEEE Sensor Array and Multichannel Signal Processing Workshop (SAM)*, pp. 1–5, July 2016.
- [21] H. V. Trees, *Optimum Array Processing (Detection, Estimation and Modulation Theory, Part IV)*. John Wiley and Sons, Inc., New York, 2002.